

# YALE PEABODY MUSEUM

P.O. BOX 208118 | NEW HAVEN CT 06520-8118 USA | PEABODY.YALE. EDU

## JOURNAL OF MARINE RESEARCH

The *Journal of Marine Research*, one of the oldest journals in American marine science, published important peer-reviewed original research on a broad array of topics in physical, biological, and chemical oceanography vital to the academic oceanographic community in the long and rich tradition of the Sears Foundation for Marine Research at Yale University.

An archive of all issues from 1937 to 2021 (Volume 1–79) are available through EliScholar, a digital platform for scholarly publishing provided by Yale University Library at <https://elischolar.library.yale.edu/>.

Requests for permission to clear rights for use of this content should be directed to the authors, their estates, or other representatives. The *Journal of Marine Research* has no contact information beyond the affiliations listed in the published articles. We ask that you provide attribution to the *Journal of Marine Research*.

Yale University provides access to these materials for educational and research purposes only. Copyright or other proprietary rights to content contained in this document may be held by individuals or entities other than, or in addition to, Yale University. You are solely responsible for determining the ownership of the copyright, and for obtaining permission for your intended use. Yale University makes no warranty that your distribution, reproduction, or other use of these materials will not infringe the rights of third parties.



This work is licensed under a Creative Commons Attribution-NonCommercial-ShareAlike 4.0 International License.  
<https://creativecommons.org/licenses/by-nc-sa/4.0/>



## **The nonlocal model of porewater irrigation: Limits to its equivalence with a cylinder diffusion model**

by Nicola J. Grigg<sup>1,2</sup>, Bernard P. Boudreau<sup>3</sup>, Ian T. Webster<sup>1</sup> and Phillip W. Ford<sup>1</sup>

### ABSTRACT

Burrows maintained by animals in aquatic sediments ventilate the sediment and can substantially alter the rates and pathways of biologically-mediated decomposition reactions. A well known and effective way of modeling the impact of such bioirrigation in sediment diagenetic models is to assume that solutes diffuse into an annulus of sediment surrounding the burrow; the reaction diffusion equations are represented in cylindrical polar co-ordinates. More commonly, bioirrigation of sediments is represented by one-dimensional “nonlocal” irrigation models. Their use is typically justified by the assertion that a nonlocal model is equivalent to a radially-integrated two-dimensional diffusion model in cylindrical-polar co-ordinates. In this paper we highlight limits to this equivalence, drawing on examples from both single-species and multiple-species reaction diffusion models. A modified derivation of the nonlocal model using a higher order Taylor series approximation was tested but found to provide little improvement over the original model. We suggest some approaches for choosing nonlocal coefficients and identify particular limitations to be alert to when applying the nonlocal model.

### 1. Introduction

Emerson *et al.* (1984) first suggested that the effects of bioirrigation could be represented in a one-dimensional diagenetic model by introducing a nonlocal (linear) exchange term. Boudreau (1984), in the same issue, demonstrated that such a nonlocal source/sink term is mathematically equivalent to a radially integrated Aller-cylinder model (Aller, 1980) under specific, if understated, conditions. Limitations to the technique have been known for some time. For example, a careful reading of Boudreau (1984) shows that his derivation applies to the case of a solute produced in the sediment and requires (1) that the lateral averaging of the reaction terms produce a meaningful and well-defined mean reaction term that can be expressed as a function of the laterally averaged concentration, and (2) that the radial dependence of the concentration can be adequately captured by the first two terms of a Taylor series.

Aller (1988) argued that interactions such as nitrification and denitrification balances

1. CSIRO Land & Water, GPO Box 1666, Canberra ACT 2601, Australia.

2. Corresponding author: *email: nicky.grigg@csiro.au*

3. Department of Oceanography, Dalhousie University, Halifax, Nova Scotia, B3H 4J1, Canada.

resulting from specific geometries may not be well described by this approximation. Furthermore, Aller (2001) concluded that a nonlocal model is only a good replacement for a full cylinder model (or a more general microenvironment model) if there is no radial dependence of reaction or transport properties, (i.e., reaction zonation around burrows cannot be important) and if the reaction kinetics are linear. These requirements are often violated in multi-component diagenetic models, which consist of multiple species interacting in nonlinear ways. Berg *et al.* (2003) recognized these limitations, pointing out in particular that if the same irrigation parameter is used for all solutes, the effects of irrigation may be overestimated for solutes that react with oxygen near the wall of a well-irrigated burrow, e.g.  $\text{NH}_4^+$ ,  $\text{Mn}^{2+}$ ,  $\text{Fe}^{2+}$  and  $\text{H}_2\text{S}$ . Berg *et al.* (2003) employed reduced irrigation parameters for affected solutes to correct for this effect.

The limitations of the nonlocal irrigation model are not well appreciated and can lead to inappropriate use of the model. Our paper aims to illustrate these limitations through a comparison of results from the cylinder and nonlocal models under some commonly encountered conditions.

## 2. The nonlocal model

We begin our development by reviewing the derivation of the nonlocal model as found in Boudreau (1984). Aller's cylinder model equation is (assuming constant porosity):

$$\frac{\partial C}{\partial t} = D_s \frac{\partial^2 C}{\partial z^2} + \frac{D_s}{r} \frac{\partial}{\partial r} \left( r \frac{\partial C}{\partial r} \right) + R(C, z, r) \quad (1)$$

where  $z$  is vertical distance from the sediment surface,  $r$  is the horizontal distance from the burrow center,  $C$  is the concentration of the species of interest,  $D_s$  is the molecular diffusion coefficient corrected for tortuosity and  $R$  is a reaction term.

At the time of its formulation (Aller, 1980),  $R$  in Eq. (1) was limited to linear kinetics with respect to the concentration  $C$ .

Typical boundary conditions for Eq. (1) are

$$\begin{aligned} C &= C_0 & z &= 0 \\ C &= C_0 & r &= r_1 \\ \frac{\partial C}{\partial r} &= 0 & r &= r_2 \\ \frac{\partial C}{\partial z} &= B & z &= L \end{aligned} \quad (2)$$

where  $r_1$  is the radius of the burrow,  $r_2$  is the outer radius of the solid annulus surrounding the burrow and  $L$  is the depth of the burrow.  $C_0$  is a known concentration at the sediment surface and  $B$  represents a prescribed flux at the base of the burrowed zone.

Following Boudreau (1984), Eq. (1) can be multiplied by  $r/(r_2^2 - r_1^2)$  and integrated laterally to give,

$$\frac{\partial \bar{C}}{\partial t} = D_s \frac{\partial^2 \bar{C}}{\partial z^2} - \frac{2D_s r_1}{r_2^2 - r_1^2} \left. \frac{\partial C}{\partial r} \right|_{r_1} + \overline{R(C, z, r)}. \quad (3)$$

The laterally averaged concentration in Eq. (3) is defined as

$$\bar{C} = \frac{2\pi \int_{r_1}^{r_2} r C dr}{2\pi \int_{r_1}^{r_2} r dr} = \frac{2}{r_2^2 - r_1^2} \int_{r_1}^{r_2} r C dr. \quad (4)$$

This laterally averaged concentration is intended to approximate the average concentration for a horizontal slice through a “cylinder” in Aller’s model. Note that the definition does not include the central tube itself.

The laterally averaged reaction term in Eq. (5) is given by

$$\overline{R(C, z, r)} = \frac{2}{r_2^2 - r_1^2} \int_{r_1}^{r_2} r R(C, z, r) dr. \quad (5)$$

Unless this averaged reaction can be expressed as an explicit function of  $\bar{C}$ ,  $r$  and  $t$ , the averaging procedure will not produce a usable model.  $\overline{R(C, r, z, t)}$  can be written in terms of  $\bar{C}$  only if it is linear in  $C$  (or is linearizable). The kinetics in Aller’s original model, and those then considered by Boudreau (1984), are indeed linear.

Boudreau (1984) next made the assumption that  $(\partial C / \partial r)|_{r=r_1}$  can be approximated by

$$\left. \frac{\partial C}{\partial r} \right|_{r=r_1} \approx \frac{\bar{C} - C_0}{\bar{r} - r_1} \quad (6)$$

where  $\bar{r}$  is the unknown radial point at which  $\bar{C}$  occurs ( $r_1 < \bar{r} < r_2$ ), i.e. that the first two terms of a Taylor series could adequately describe the gradient between the solute concentration at the tube wall and the mean concentration that occur at a radial distance  $\bar{r}$ .

As a result of the two assumptions expressed by Eqs. (5) and (6), the radially averaged concentration will obey a one-dimensional reaction-diffusion equation of the form

$$\frac{\partial \bar{C}}{\partial t} = D_s \frac{\partial^2 \bar{C}}{\partial z^2} - \alpha(\bar{C} - C_0) + R(\bar{C}, z) \quad (7)$$

where

$$\alpha(z) \equiv \frac{2D_s r_1}{(r_2^2 - r_1^2)(\bar{r} - r_1)}. \quad (8)$$

The second term on the right-hand side of Eq. (7) constitutes an apparent source/sink that accounts for the effects of 3-D irrigation. Because the term is driven by the

concentration difference,  $\bar{C}(z) - C_0$ , which generally refers to nonadjacent points, it is called a nonlocal transport. Physically this term accounts for irrigation by allowing exchange of water between any depth  $z$  in the irrigated zone and the overlying water.

Eq. (6) can be replaced with a higher-order approximation to the radial concentration gradient at the burrow wall. Rather than adopting a linear approximation, taking the next highest order Taylor series expansion amounts to assuming that the concentration profile is a quadratic (three unknown parameters) with the following conditions providing three equations:  $C(r_1) = C_0$ ;  $C(\bar{r}) = \bar{C}$ ; and  $\partial C(z, r)/\partial r|_{r_2} = 0$ . Solving this system yields:

$$\left. \frac{\partial C}{\partial r} \right|_{r_1} = \frac{2(r_2 - r_1)}{(r_1 - \bar{r})(2r_2 - \bar{r} - r_1)} (C_0 - \bar{C}). \quad (9)$$

In which case Eq. (8) is replaced with

$$\alpha(z) = \frac{4D_s r_1}{(r_2 + r_1)(r_1 - \bar{r})(2r_2 - \bar{r} - r_1)}. \quad (10)$$

We will address three points in this paper:

- 1) To what extent are the approximations in Eqs. (6) and (9) accurate, and can they be improved?
- 2) According to Eq. (8),  $\alpha$  is a function of diffusivity and  $\bar{r}$ , both of which differ between chemical species, and can both be functions of depth. Given it is common practice simply to use the same  $\alpha$  value across many species and at all depths in a model, is this simplification valid?
- 3) Integrating the reaction term is only possible if reaction kinetics are linear and independent of the concentration of other species. How well does this approach work for a set of coupled nonlinear differential equations, as is typical for multiple species diagenesis models?

### 3. The comparator 3-D models

Each of our questions is answered by making direct comparisons between solutions to the full cylinder model and nonlocal model. To answer the first two questions, we drew on cylinder model results from Aller (1980). The reaction terms in this example are linear, allowing us to test just one of the assumptions underlying the equivalence between cylinder and nonlocal models, i.e., the approximation to the radial concentration gradient. To address our third question, regarding the implications of averaging the nonlinear reaction term, we coupled a nitrogen dynamics model—based on Blackburn and Blackburn (1993)—to a cylindrical burrow irrigation model.

a. *Analytical solutions from Aller (1980)*

Aller (1980) employed the cylinder model with the following reaction term

$$R(C, z) = k(C_{eq} - C) + R_0 \exp(-\eta z) + R_1 \quad (11)$$

to model the sediment-water exchange of sulfate ( $\text{SO}_4^{2-}$ ), ammonium ( $\text{NH}_4^+$ ) and dissolved silica (DSi), where  $k$ ,  $R_0$ ,  $\eta$  and  $R_1$  are empirical constants and  $C_{eq}$  is an equilibrium concentration. The steady state analytical solution to the cylinder model is (Aller, 1980):

$$C(z, r) = C_0 + Bz + \frac{2}{LD_s} \sum_{n=0}^{\infty} \frac{G_n}{\mu_n^2} \left[ \frac{U_0(\mu_n r)}{U_0(\mu_n r_1)} - 1 \right] \sin(\lambda_n z) - \frac{2B}{L} \sum_{n=0}^{\infty} \frac{(-1)^n U_0(\mu_n r)}{\lambda_n^2 U_0(\mu_n r_1)} \sin(\lambda_n z) \quad (12)$$

where

$$n = 0, 1, 2, \dots$$

$$\lambda_n = \left( n + \frac{1}{2} \right) \frac{\pi}{L}$$

$$\mu_n = \left( \frac{k}{D_s} + \lambda_n^2 \right)^{1/2}$$

$$G_n = \frac{k(C_0 - C_{eq})}{\lambda_n} - \frac{R_1}{\lambda_n} + \frac{(-1)^n kB}{\lambda_n^2} + \frac{R_0((-1)^n \eta \exp(-\eta L) - \lambda_n)}{(\eta^2 + \lambda_n^2)}$$

$$U_0(\mu_n r) = K_1(\mu_n r_2) I_0(\mu_n r) + I_1(\mu_n r_2) K_0(\mu_n r)$$

and  $I_v(z)$  and  $K_v(z)$  are the modified Bessel functions of the first and second kind, respectively, of order  $v$ . Aller (1980) set parameters to the values shown in Table 1 (with only  $r_2$  used as a fitting parameter) and found excellent agreement between modeled and field profiles.

b. *Numerical multi-species nitrogen model*

We implemented a multi-species nitrogen cycling model using Aller's cylinder model burrow geometry, Eq. (1). Such a model is appropriate for investigating nitrification-denitrification interactions in the sediment. Five chemical species, oxygen ( $\text{O}_2$ ), nitrate ( $\text{NO}_3^-$ ), dissolved organic carbon (DOC), ammonium ( $\text{NH}_4^+$ ) and nitrogen gas ( $\text{N}_2$ ) were modeled using the kinetics based on those described in Blackburn and Blackburn (1993). Twelve species were represented in their model: carbon dioxide ( $\text{CO}_2$ ), dissolved organic carbon (DOC), dissolved organic nitrogen (DON), sulfide ( $\text{HS}^-$ ), adsorbable ammonium ( $\text{NH}_{4\_ex}$ ),  $\text{NO}_3^-$ ,  $\text{N}_2$ , particulate organic carbon (POC), particulate organic nitrogen (PON),

Table 1. The cylinder model parameters used in Aller (1980).

Variable	SO <sub>4</sub> <sup>2-</sup>	NH <sub>4</sub> <sup>+</sup>	DSi
$C_0$	14.7 mM	0.0002 mM	0.074 mM
$B$	-0.1 mM cm <sup>-1</sup>	0.011 mM cm <sup>-1</sup>	0.060 mM cm <sup>-1</sup>
$D_s$	0.717 cm <sup>2</sup> d <sup>-1</sup>	1.33 cm <sup>2</sup> d <sup>-1</sup>	0.687 cm <sup>2</sup> d <sup>-1</sup>
$\eta$	0.36 cm <sup>-1</sup>	0.61 cm <sup>-1</sup>	0
$R_0$	-0.383 mM d <sup>-1</sup>	0.267 mM d <sup>-1</sup>	0
$R_1$	-0.061 mM d <sup>-1</sup>	0.0081 mM d <sup>-1</sup>	0
$k$	0	0	0.2 d <sup>-1</sup>
$C_{eq}$	—	—	0.577 mM
$r_1$	0.05 cm	0.05 cm	0.05 cm
$r_2$	2.1 cm	2.1 cm	2.1 cm
$L$	15 cm	15 cm	15 cm

O<sub>2</sub> and sulfate (SO<sub>4</sub><sup>2-</sup>). The reasons for omitting seven of the species are varied. The evolution of nitrogen species PON and DON can be approximated from carbon by assuming a fixed C:N ratio. An explicit POC concentration was replaced with a production rate of DOC ( $P_{DOC}$ ) which specifies the rate and distribution of DOC production. CO<sub>2</sub> was omitted, as its exclusion does not affect the distributions of other species. A model version was constructed which included adsorbable ammonium, however there was negligible difference in results when it was excluded from the model. The authors of the original model have also routinely omitted adsorbable NH<sub>4</sub><sup>+</sup> from their model formulation. A model version was constructed with HS<sup>-</sup> and SO<sub>4</sub><sup>2-</sup> included, and their exclusion was found to have little influence on the results for this application. Reduction of DOC by SO<sub>4</sub><sup>2-</sup> is included in the model without explicitly modeling the concentration of SO<sub>4</sub><sup>2-</sup> (i.e. we assume there is excess SO<sub>4</sub><sup>2-</sup>).

The expressions for the reaction rates of the remaining species are:

$$\begin{aligned}
 R_{O_2} &= -k_3 O_{2\_stim}[DOC] - 2k_6 O_{2\_stim}[NH_4^+] \\
 R_{NO_3^-} &= -k_4 NO_{3\_stim} O_{2\_inhib}[DOC] + k_6 O_{2\_stim}[NH_4^+] \\
 R_{DOC} &= P_{DOC} - k_3 O_{2\_stim}[DOC] \\
 &\quad - 2k_5 SO_{4\_stim} O_{2\_inhib}[DOC] - 1.25k_4 NO_{3\_stim} O_{2\_inhib}[DOC] \\
 R_{N_2} &= 0.5k_4 NO_{3\_stim} O_{2\_inhib}[DOC] \\
 R_{NH_4^+} &= k_3 O_{2\_stim} \frac{[DOC]}{\lambda_{CN}} + 1.25k_4 NO_{3\_stim} O_{2\_inhib} \frac{[DOC]}{\lambda_{CN}} \\
 &\quad + 2k_5 SO_{4\_stim} O_{2\_inhib} \frac{[DOC]}{\lambda_{CN}} - k_6 O_{2\_stim}[NH_4^+]
 \end{aligned} \tag{13}$$

where square brackets represent porewater concentration, and  $\lambda_{CN}$  is the carbon to nitrogen ratio (assumed to follow Redfield C:N stoichiometry of 106:16). The rate constants are the same as those specified by Blackburn and Blackburn (1993):  $k_3 = 30 \text{ d}^{-1}$  for DOC oxidation by  $\text{O}_2$ ;  $k_4 = 30 \text{ d}^{-1}$  for DOC oxidation by  $\text{NO}_3^-$ ;  $k_5 = 5 \text{ d}^{-1}$  for DOC oxidation by  $\text{SO}_4^{2-}$ ;  $k_6 = 30 \text{ d}^{-1}$  for  $\text{NH}_4^+$  oxidation by  $\text{O}_2$  (nitrification);  $k_7 = 200 \text{ d}^{-1}$  for  $\text{HS}^-$  oxidation by  $\text{O}_2$ . The stimulation and inhibition functions are:

$$C_{\text{stim}} = \begin{cases} [C]/C_{\text{crit}} & \text{if } [C] < C_{\text{crit}} \\ 1 & \text{otherwise} \end{cases} \quad (14)$$

$$\text{O}_{2\text{inhib}} = \begin{cases} 1 - [\text{O}_2]/C_{\text{crit}} & \text{if } [\text{O}_2] < C_{\text{crit}} \\ 0 & \text{otherwise} \end{cases}$$

where  $C_{\text{crit}}$  is  $30 \text{ nmol cm}^{-3}$ .  $\text{SO}_{4\text{stim}}$  is an exception, and is simply given a value of 1.

The model was solved in Matlab, using the method of lines (Boudreau, 1997). The cylindrical-polar diffusion equation was represented by a central finite difference approximation in space, hence reducing the system of coupled partial differential equations to a set of ordinary differential equations (ODEs). The model allowed for a finer grid to be prescribed at the burrow wall, so providing greater spatial resolution at this interface. At the interface between two grid sizes, second order finite difference formulas for an uneven grid were used (Boudreau, 1997, p. 326). Matlab's stiff ODE solver, "ode15s," was used to solve the system of equations. The solver's performance was improved by specifying a sparse analytical Jacobian matrix for the system of equations, and modifying "ode15s" to perform a column permutation prior to any LU decompositions (matrix decomposition to a product of upper and lower triangular matrices).

#### 4. Results and discussion

##### a. Validity of approximating the gradient at the burrow wall

Eq. (6) will constitute a reasonable approximation of the gradient at the burrow wall if higher-order derivatives are not significant. This point is illustrated in Figure 1. The solid line is the actual radial solute profile (at an arbitrary  $z$ ). The line labeled "a" is the extension of the slope (gradient) of this profile at the tube wall,  $r = r_1$ . The line labeled "b" is the linear gradient predicted by Eq. (6). The top diagram, Figure 1A, illustrates the case where higher-order derivatives have only a modest influence; line b is then a passable approximation to line a, and application of Eq. (6) would be appropriate. The bottom diagram, Figure 1B, displays the situation when the profile has strong curvature in the slope; under this condition, line b is not a reasonable approximation to the actual wall slope, line a. If we employ (9) instead of Eq. (6), the comparison is between a quadratic that links  $C(r_1, z)$  and  $\bar{C}$ , rather than a linear function, but the argument is identical.

Which of the diagrams in Figure 1 best describes natural sediments? To answer this question we examined the examples used in Aller (1980), i.e., a prototypical nearshore mud; the solutions for ammonium ( $\text{NH}_4^+$ ), sulfate ( $\text{SO}_4^{2-}$ ) and dissolved silica (DSi) are



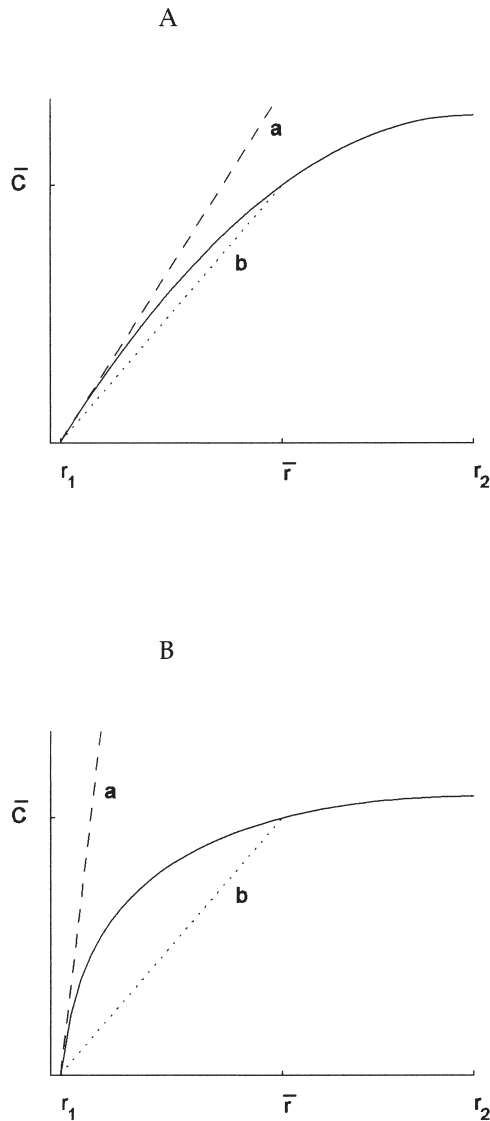


Figure 1. Hypothetical solute profiles (solid lines) with a weak radial gradient (A) and a strong radial gradient (B). The dashed lines (a) in both diagrams are the extensions of the initial (wall) gradients, while the dotted lines (b) are the predicted initial gradients assuming a two-term Taylor series between the initial wall concentration and the radially averaged concentration.

shown in Figure 2. The dotted lines in the figures plot  $\bar{r}$ , i.e., the radial coordinate of  $\bar{C}$  at each depth for each of these species. For all three solutes,  $\bar{r}$  is located roughly midway between  $r_1$  and  $r_2$ . The radial concentration gradients are steepest at the burrow wall,  $r = r_1$ , and a visual inspection of the data suggests that the concentration gradient between  $r_1$

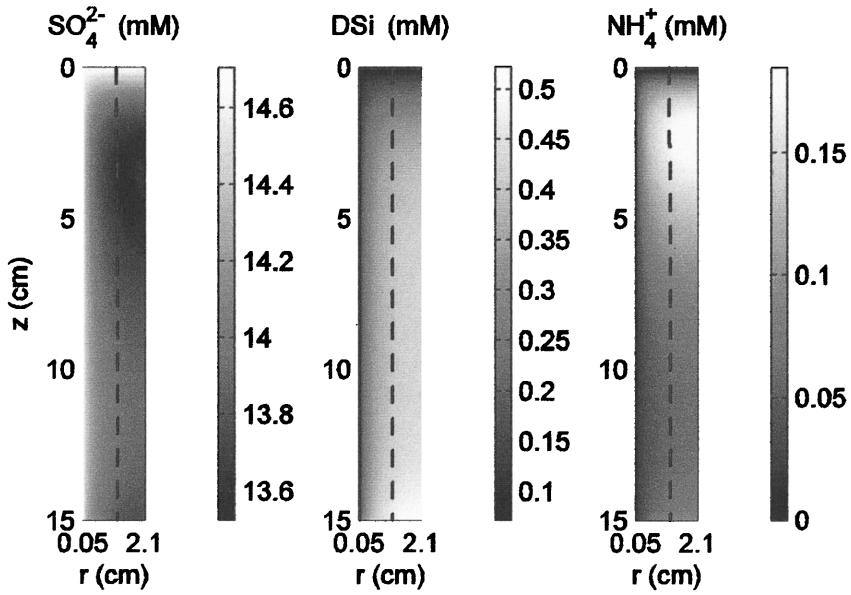


Figure 2. Concentration distributions of  $\text{SO}_4^{2-}$ , DSi and  $\text{NH}_4^+$  calculated from Eq. (12) using the model parameters in Table 1. The dotted line plots  $\bar{r}$ .

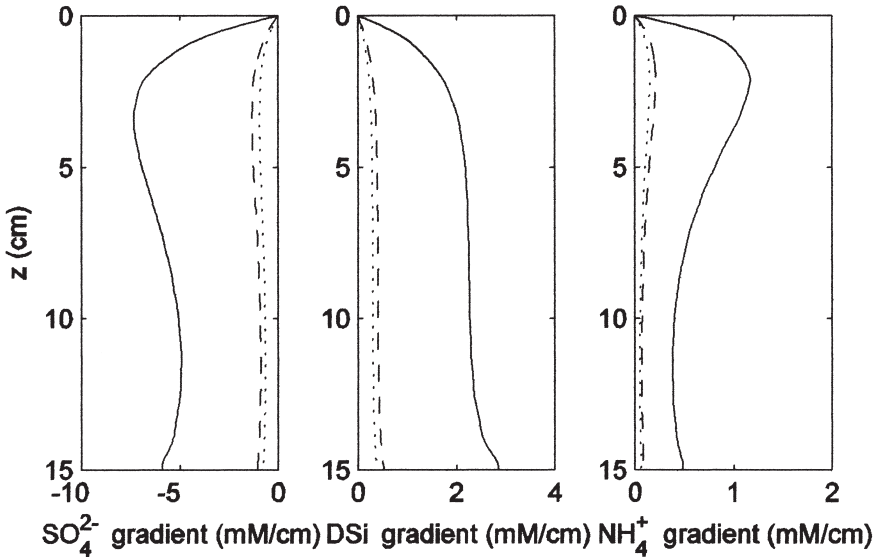


Figure 3. Comparison between the analytical radial derivative at  $r_1$  (solid line), the approximation given in Eq. (6) (dotted line) and the higher order approximation given in Eq. (9) (dash-dot line).

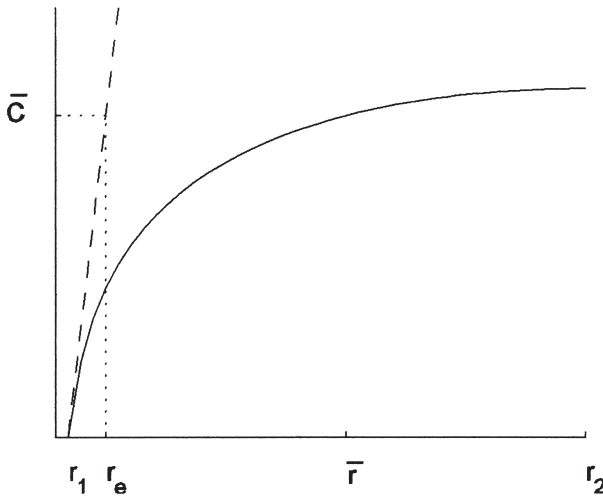


Figure 4. Illustration of the approximation of the initial wall gradient by Eq. (15).  $r_e$  is the radial distance where the extension of the initial gradient would encounter the radially averaged concentration of the profile.

and  $\bar{r}$  is appreciably nonlinear. Figure 3 provides a visual comparison between the analytical radial derivative at  $r = r_1$  and the approximations given by Eqs. (6) and (9) as a function of depth for this same example. (To create this figure, Eqs. (8) and (10) were used to calculate two  $\alpha(z)$  profiles, and Matlab’s “ode15s” function was used to find a steady state numerical solution to the nonlocal model, Eq. (7), using these  $\alpha$  profiles.) Note that the Taylor series approximations in Eqs. (6) and (9) grossly underestimate the actual gradient, i.e., the situation is characterized by Figure 1B.

If Eq. (6) is not an acceptable approximation to the gradient at the wall, is there a likely acceptable linear approximation that involves only  $\bar{C}$  and  $C_0$ ? This latter restriction is needed because we cannot afford to introduce another unknown concentration and hope for a useful formula. The positive answer to this question is illustrated in Figure 4. The linear extension of the initial gradient contains a point that has a corresponding concentration  $\bar{C}$ ; thus,  $(\bar{C} - C_0)/(r_e - r_1)$  constitutes a reasonable linear approximation,

$$\left. \frac{\partial C}{\partial r} \right|_{r_1} = \frac{\bar{C} - C_0}{r_e - r_1}. \tag{15}$$

The objection to this equation would be that  $r_e$  is unknown, but remember that  $\bar{r}$  was also an unknown, and this was not an impediment to the application of the nonlocal irrigation model. With Eq. (15), the exchange coefficient adopts the altered definition

$$\alpha \equiv \frac{2D_s r_1}{(r_2^2 - r_1^2)(r_e - r_1)} \tag{16}$$

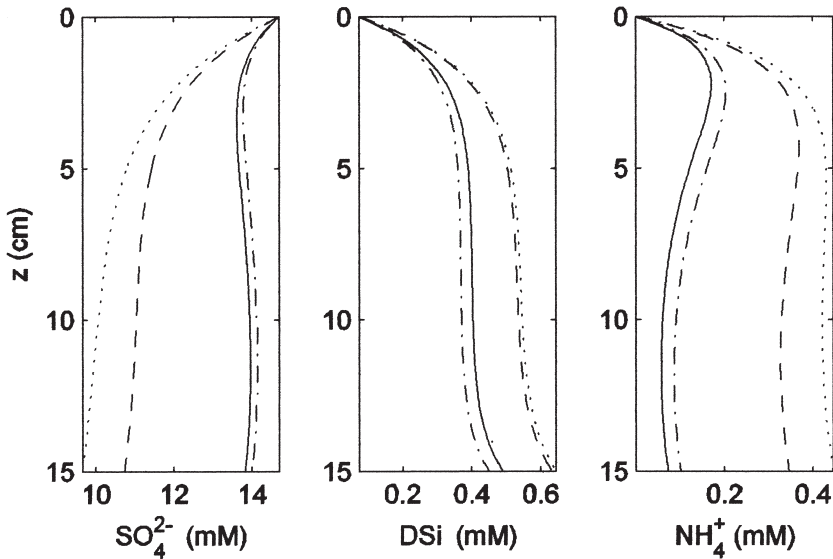


Figure 5. Comparison between the average concentration profile calculated from Eq. (12) (solid line) and the steady state numerical solution to Eq. (7) using Eq. (8) to calculate  $\alpha$  (dotted line) and Eq. (10) to calculate  $\alpha$  (dashed line). A process of trial and error was also used to find a single value of  $\alpha$  that provided a good match across all three species (dash-dot line,  $\alpha = 0.14$ ).

and following the derivation in Boudreau (1984), irrigation again appears as a nonlocal source-sink for solutes that meet the other relevant conditions. While both  $\bar{r}$  and  $r_e$  can, in principle, be calculated from the solution of the 3-D tube model, in practice both are unknown and  $\alpha$  is a fitting parameter.

#### b. Validity of using a constant value for $\alpha$

The most common application of Eq. (7) assumes that  $\alpha$  is a constant across all chemical species and at all depths. Values of  $\alpha$  are found by calibration against measured profiles, and the expression given in Eq. (8) is rarely used in practice, although it has been employed by Furukawa *et al.* (2000) and Koretsky *et al.* (2002). Treating  $r_e$  in Eq. (16) as a free fitting parameter that is the same for each species (while retaining different  $D_s$  values for each species), we found that  $r_e = 0.2$  cm yields values of  $\alpha_{\text{SO}_4} = 0.11 \text{ d}^{-1}$ ,  $\alpha_{\text{Si}} = 0.10 \text{ d}^{-1}$  and  $\alpha_{\text{NH}_4} = 0.20 \text{ d}^{-1}$  which produce profiles that are visually indistinguishable from the radially-averaged analytical solutions. It should be noted that the value of  $\alpha$  differs for each species as they each have different  $D_s$  values, but they are derived from a common  $r_e$ . If the same value of  $\alpha$  ( $\alpha = 0.14 \text{ d}^{-1}$ ) is used for all three species, the match between the two models is still good, but less convincing—see Figure 5. The implication is that the use of a single value of  $\alpha$  is not necessarily valid for multiple species models.

Given that useful values of  $\alpha$  do exist, an alternative method for finding them could be to

evaluate a one-dimensional radial model, calculate the radial gradient at the burrow wall and then calculate a value of  $\alpha$  that would make the following expression true:

$$\alpha(\bar{C} - C_0) = \frac{2D_s}{r_2^2 - r_1^2} r_1 \left. \frac{\partial C}{\partial r} \right|_{r=r_1}. \quad (17)$$

The steady state equation for the one-dimensional radial model is

$$\frac{D_s}{r} \frac{\partial}{\partial r} r \frac{\partial C}{\partial r} + R(C, r) = 0. \quad (18)$$

For zeroth order reaction kinetics,  $R = R_1$ , the analytical solution is

$$C(r) = \frac{-R_1}{4D_s} r^2 + \frac{R_1 r_2^2}{2D_s} \ln(r) + C_0 + \frac{R_1 r_1^2}{4D_s} - \frac{R_1 r_2^2}{2D_s} \ln(r_1). \quad (19)$$

For first order reaction kinetics,  $R = k(C_{eq} - C)$ , the analytical solution is

$$C = A_1 I_0(\mu r) + A_2 K_0(\mu r) + C_{eq} \quad (20)$$

where  $A_1$ ,  $A_2$  and  $\mu$  are constants

$$A_1 = \frac{(C_0 - C_{eq})K_1(\mu r_2)}{U(\mu r_1)}$$

$$A_2 = \frac{(C_0 - C_{eq})I_1(\mu r_2)}{U(\mu r_1)} \quad (21)$$

$$\mu = \sqrt{k/D_s}$$

$$U(\mu r) = K_1(\mu r_2)I_0(\mu r) + I_1(\mu r_2)K_0(\mu r).$$

These latter expressions can be used to compare the analytical radial profiles with the linear and quadratic approximations underlying the derivations of Eqs. (8) and (10)—see Figure 6. The  $\alpha$  values calculated using Eq. (7), with the analytical solutions to Eq. (18) providing the radial gradient and  $\bar{C}$ , are a close match to those found by fitting  $r_e$  as a free parameter, i.e. alternative values of  $\alpha_{\text{SO}_4} = 0.11 \text{ d}^{-1}$ ,  $\alpha_{\text{Si}} = 0.11 \text{ d}^{-1}$  and  $\alpha_{\text{NH}_4} = 0.20 \text{ d}^{-1}$ .

### c. Application to a multiple-species system

The analysis so far has been limited to single-species models with reaction terms that are easily integrated radially. Sediment diagenesis models are typically coupled multiple-species models. In such models the reaction terms are more complicated, and because they are dependent on other species' concentrations, they are likely to vary appreciably with  $r$ .

The cylinder model was run with the same burrow geometry as earlier examples. A

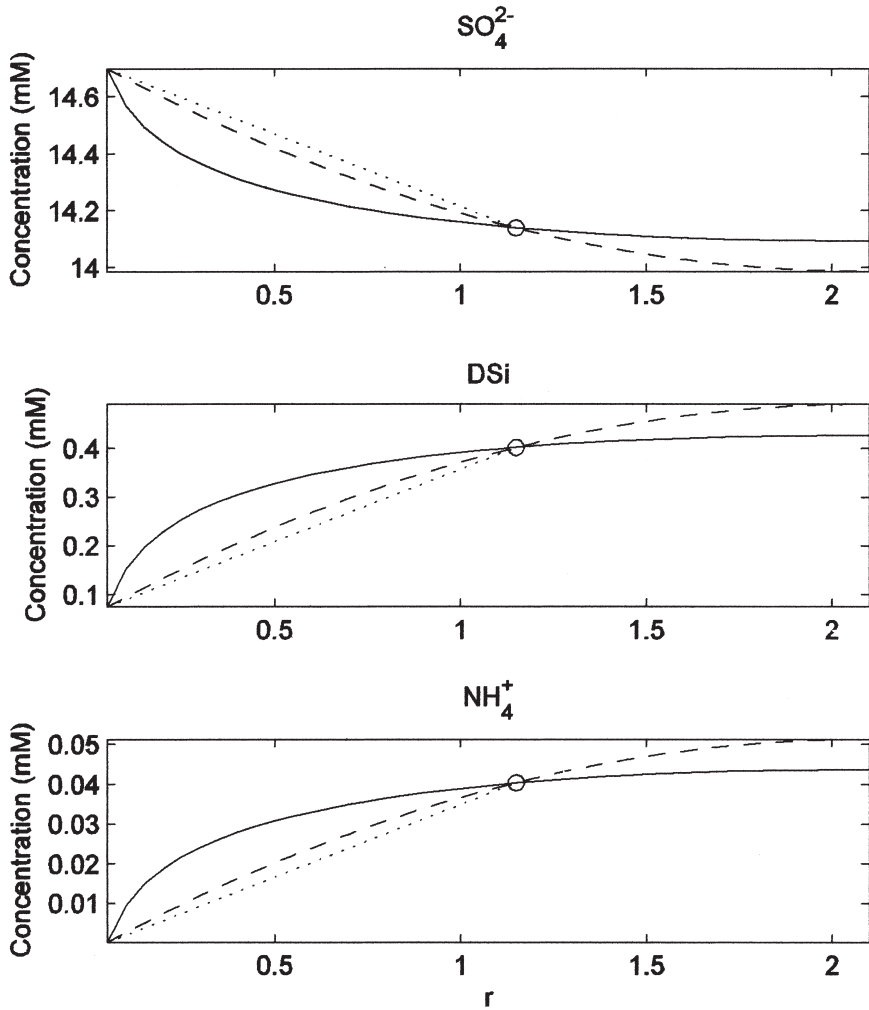


Figure 6. Analytical solutions to 1D radial diffusion model (solid line) compared with linear (dotted line) and quadratic (dashed line) approximations. Circles mark the location of  $(\bar{r}, \bar{C})$ .

40-day run was sufficient to bring the cylinder model solution to steady state.  $P_{\text{DOC}}$  was uniformly distributed with a value of  $200 \text{ nmol cm}^{-3} \text{ d}^{-1}$ , which corresponds to a carbon mineralization rate of  $25.5 \text{ mmol m}^{-2} \text{ d}^{-1}$  for this burrow geometry, assuming  $P_{\text{DOC}}$  is zero below the burrowed zone of sediment. A zero flux boundary condition was prescribed at the maximum  $z$  value. Figure 7 illustrates the steady state concentration distributions from this configuration.

The original derivation for  $\alpha$ , Eq. (8), produced a poor fit to the model profiles. Using a one-dimensional radial model and calculating  $\alpha$  from Eq. (17) provided an improved

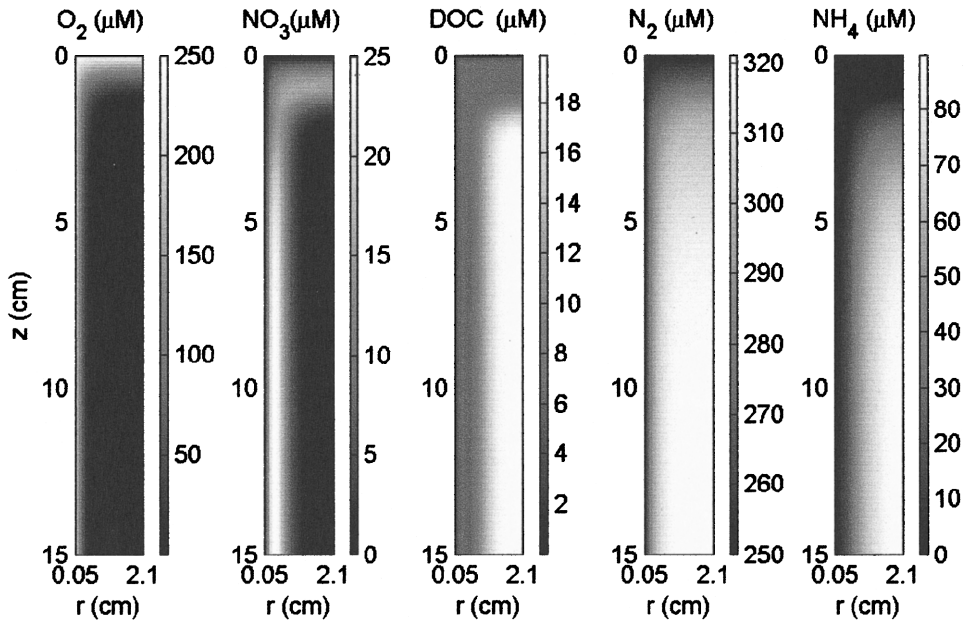


Figure 7. Two-dimensional steady-state concentration distributions from the 5-species nitrogen cycling model.

match. The best match was found by treating  $r_e$  as a free parameter in Eq. (16) and substituting the value for  $r_e$  found in the previous single-species examples for this geometry,  $r_e = 0.2$  cm—see Figure 8.

These last two cases demonstrate a trade-off that is faced when dealing with nonlinear reaction terms. Calculating  $\alpha$  from Eq. (17) ensures that radial gradient implicit in  $\alpha$  matches the burrow wall gradient in the cylinder model. Yet this calculation yields a poorer match than the second approach, where a single  $r_e$  value is treated as a free parameter in Eq. (16). Plotting the  $r_e$  and  $\bar{C}$  values on the radial profiles for each species demonstrates that this second approach yields a poorly matched radial gradient at the burrow wall for  $NH_4^+$  and  $NO_3^-$  (Fig. 9), yet it produces a better match to the radially-averaged concentration profiles for these species (Fig. 8). A consequence of the nonlinear reaction term is that it is impossible to match both the radial gradient implicit in  $\alpha$  and the radially-averaged concentration profiles simultaneously. This example demonstrates that this kind of problem is likely to affect species that have a strong radial dependence in their reaction rate (e.g. in this particular case the thin nitrification zone leads to a nitrate maximum in a narrow zone near the burrow wall, and the consumption of  $NH_4^+$  in the oxic zone leads to a flattened  $NH_4^+$  gradient close to the burrow wall). One can imagine even worse situations where a linear extrapolation from  $r_1$  would not even intersect a value of  $\bar{C}$  over the whole annulus (e.g. if there is a zero flux or reversal in the sign of the gradient due to strong

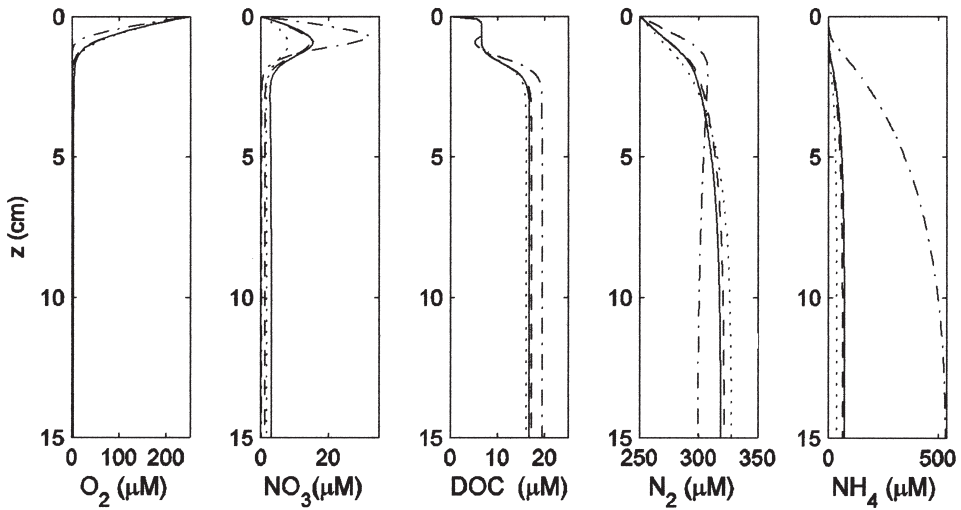


Figure 8. Comparison between the cylinder model (solid line) and nonlocal model with three alternative derivations of  $\alpha$ : Eq. (8) (dash-dot line); Eq. (8) but modified so that  $r_e$  is a fitting parameter and takes the value  $r_e = 0.2$  (dashed line); and using a one-dimensional radial model to calculate  $\alpha$  from Eq. (17) (dotted line).

consumption or production in the zone at the burrow wall). The inability to match both the gradient implicit in  $\alpha$  and average concentrations has implications for flux calculations, as discussed below. The remaining discussion on the nonlocal model refers to the case where  $\alpha$  has been derived from Eq. (16) using  $r_e = 0.2$  cm. Eq. (7) assumes that  $\overline{R(C, r, z)} = R(\overline{C}, z)$  is a reasonable approximation; yet in the nitrogen model the reaction terms are coupled and nonlinear. A comparison between  $\overline{R(C, r, z)}$  and  $R(\overline{C}, z)$  profiles demonstrates that they are indeed very different (Fig. 10) which makes the good match between nonlocal and cylinder model concentrations even more surprising. In fact, although the absolute differences between the nonlocal and radially-averaged concentrations are low, there are some substantial relative differences between the concentrations for  $O_2$  (and to a lesser extent,  $NO_3^-$ ). At depth, the radially averaged  $O_2$  concentrations are more than a factor of 7 higher than the nonlocal values. This difference is enough to ensure that  $R(\overline{C}, z)$  is much closer to  $\overline{R(C, r, z)}$  than might be expected.

The generation of accurate sediment profiles is useful; however, the goal of many sediment diagenesis models is to link the sediment dynamics to the water column by inferring fluxes between the two systems. The cylinder model flux formulae as modified from Aller (1980) to represent the flux per unit of planar sediment surface are then given by:

$$J_{\text{cyl}} = J_z + J_r \quad (22)$$



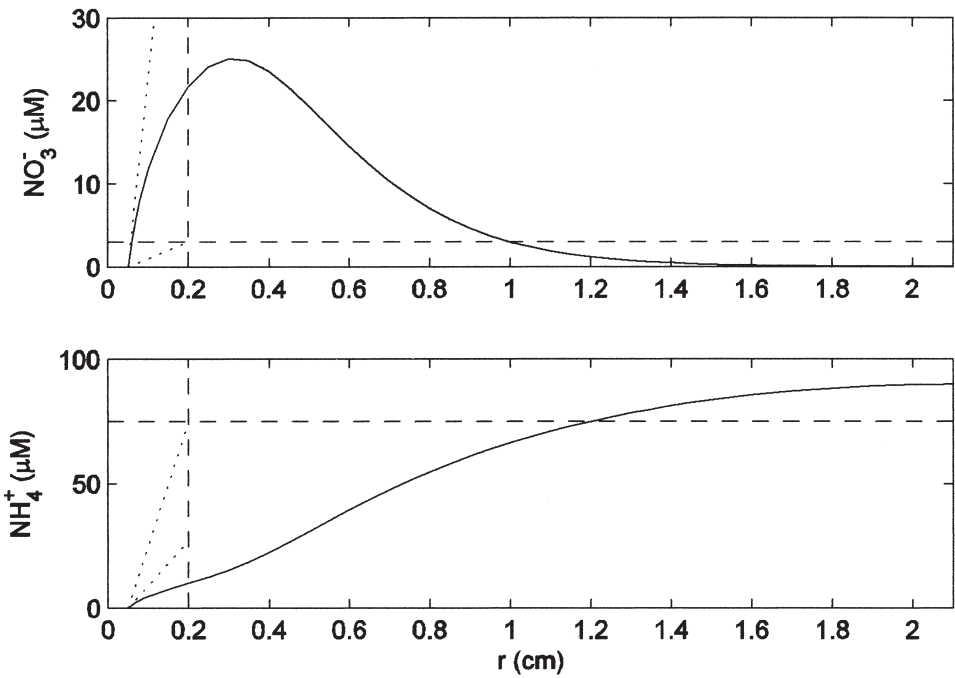


Figure 9. Radial profiles at the base of the cylinder model ( $z = L$ ) for  $\text{NO}_3^-$  and  $\text{NH}_4^+$ . Dashed lines show the location of  $r_e$  and  $\bar{C}$ . Dotted lines show the actual gradient at  $r_1$  and the gradient assumed by the choice of  $r_e$ .

where

$$J_z \equiv - \frac{2\pi\phi D_s \int_{r_1}^{r_2} \left. \frac{\partial C}{\partial z} \right|_{z=0} r dr}{2\pi \int_{r_1}^{r_2} r dr}$$

$$J_r \equiv - \frac{A_r \phi D_s \int_0^L \left. \frac{\partial C}{\partial r} \right|_{r=r_1} dz}{A_z \int_0^L dz}$$

and  $A_z$  is the surface area of the cylinder top at  $z = 0$  and  $A_r$  is the surface area of the burrow wall.

Because the system is at steady state and there is no advection, the total flux for a species can also be found by integrating that species' reaction term:

$$J_{\text{cyl}} = \frac{2 \int_0^L \int_{r_1}^{r_2} \phi R r dr dz}{r_2^2 - r_1^2}. \tag{23}$$

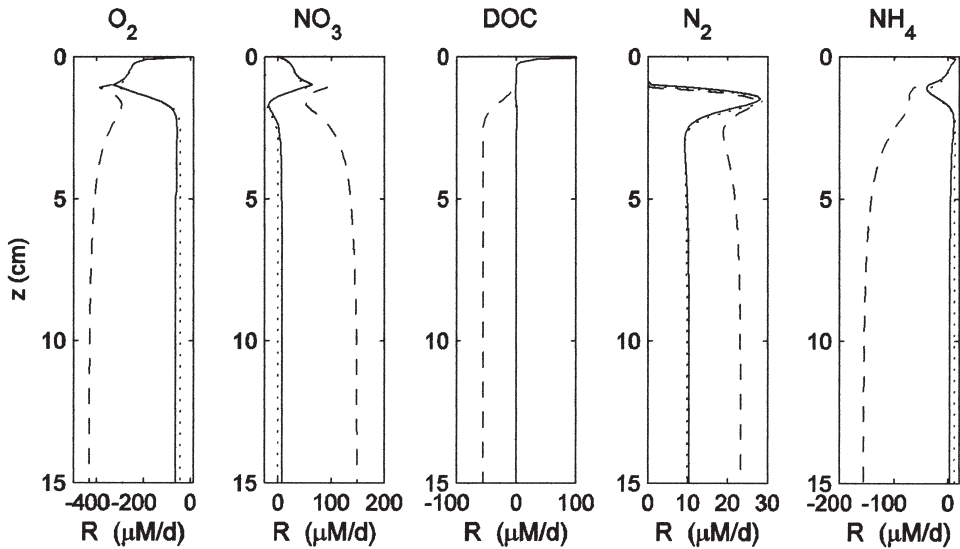


Figure 10. Comparison between reaction profiles. Solid line:  $\overline{R(C, z, r)}$ , where  $C$  is the concentration distribution from the cylinder model; Dashed line:  $R(\overline{C}, z)$  where  $\overline{C}$  is the radially-averaged concentration calculated from the cylinder model; Dotted line:  $R(\overline{C}, z)$ , where  $\overline{C}$  is the concentration profile produced by the nonlocal model (as shown in Fig. 8).

If the total flux between the sediment and overlying water is to be predicted with the nonlocal model, the diffusive flux across the sediment boundary and an integrated nonlocal flux term needs to be included in the calculation:

$$J_{nl} = -\phi D_s \left. \frac{\partial \overline{C}}{\partial z} \right|_{z=0} - \int_0^L \phi \alpha (\overline{C} - C_0) dz. \quad (24)$$

Fluxes predicted from the two-dimensional and nonlocal models are significantly different for some species (Table 2). In particular, the  $\text{NH}_4^+$  flux is more than four times higher in the nonlocal model, and the  $\text{NO}_3^-$  flux is 26% of the value predicted by the cylinder model.

## 5. Conclusion

The equivalence between nonlocal and cylinder models derived by Boudreau (1984) rests on two key assumptions: that a Taylor series approximation to the radial concentra-

Table 2. Fluxes predicted from the cylinder and nonlocal models ( $\text{mmol m}^{-2} \text{d}^{-1}$ ).

	O <sub>2</sub>	NO <sub>3</sub> <sup>-</sup>	DOC	N <sub>2</sub>	NH <sub>4</sub> <sup>+</sup>
Cylinder model flux ( $J_{\text{cyl}}$ )	-10.5	0.97	0.16	1.30	0.25
Nonlocal model flux ( $J_{\text{nl}}$ )	-8.47	0.25	0.14	1.26	1.05
$J_{\text{nl}}/J_{\text{cyl}}$	0.80	0.26	0.90	0.97	4.21

tion gradient is valid, and that nonlinear reaction terms can be radially averaged and take the same functional form, i.e.  $\overline{R(C, r, z)} = R(\bar{C}, z)$ . Using analytical solutions to the full cylinder model drawn from Aller (1980), we have demonstrated that the radial concentration gradient profiles are poorly approximated with both linear and quadratic Taylor series approximations. Further, applying the derived  $\alpha$  profiles in a nonlocal model yields a poor match to the radially averaged cylinder model solutions. We conclude that using Eq. (8) or (10) to calculate  $\alpha(z)$  may not yield results that match the cylinder model, and the poor match is solely due to the poor Taylor series approximation to the radial gradient, as reaction kinetics were linear in these examples.

We have also found that for applications with linear reaction rates, meaningful  $\alpha$  values are possible by replacing the Taylor series approximation, Eq. (6), with an approximation based on a linear extension of the initial gradient, Eq. (15).  $\bar{r}$  is then replaced by the radial distance,  $r_e$ , at which the extension of the initial gradient reaches the radially averaged concentration  $\bar{C}$ . The exchange parameter  $\alpha$  is then defined by Eq. (16), which can be calculated as a fitting parameter to data or from a one-dimensional radial model using Eq. (17).

Greater challenges are faced when attempting to model multiple-species systems containing coupled nonlinear reaction terms. Using a one-dimensional radial model to find  $\alpha$  values produced an improved fit over using Eq. (8); however the match was still poor. Substituting the fitted  $r_e$  value from the single-species examples into Eq. (8) yielded the best results; however, the reaction rate profiles and fluxes produced by the nonlocal and cylinder models still differed. We conclude that when modeling reactions with a strong radial dependence in reaction rates (e.g. where substantial production or consumption occurs in a narrow band near the burrow wall), it cannot be assumed that a nonlocal model will give the same results as the cylinder model.

It should be emphasized that the nonlocal irrigation model's performance differs from the cylinder model only under quite specific circumstances discussed above. The model remains ideally suited to modeling inert tracers or species with simple reaction kinetics, so long as some effort is made to justify the choice of nonlocal parameter. It would also be misleading to suggest that the cylinder model is the ideal standard against which all other models should be assessed. Both models are only approximations of complicated processes, and indeed there are likely to be circumstances where a nonlocal model might be more appropriate than a cylinder model (e.g. rapid episodic advective fluxes between sediment and overlying water).

*Acknowledgments.* This work formed part of the first author's Ph.D. research at CSIRO Land and Water and the Centre for Resource and Environmental Studies, Australian National University. Her ANU supervisor was Ian White and she was supported by a Commonwealth Government Australian Postgraduate Award. BPB was supported by US ONR Contract #N00014-99-1-0063 and #N00014-02-1-0107.

We would like to thank Barbara Robson, Karen Wild-Allen and two anonymous reviewers for their helpful comments and suggestions.

## REFERENCES

- Aller, R. C. 1980. Quantifying solute distributions in the bioturbated zone of marine sediments by defining an average microenvironment. *Geochim. Cosmochim. Acta*, *44*, 1955–1965.
- 1988. Benthic fauna and biogeochemical processes in marine sediments: The role of burrow structures, *in* Nitrogen Cycling in Coastal Marine Environments, T. H. Blackburn and J. Sorensen, eds., Wiley, United Kingdom, 451 pp.
- 2001. Transport and reactions in the bioirrigated zone, *in* The Benthic Boundary Layer: Transport Processes and Biogeochemistry, B. P. Boudreau and B. B. Jørgensen, eds., Oxford University Press, NY, 418 pp.
- Berg, P., S. Rysgaard and B. Thamdrup. 2003. Dynamic modeling of early diagenesis and nutrient cycling. A case study in an arctic marine sediment. *Am. J. Sci.*, *303*, 905–955.
- Blackburn, N. D. and T. H. Blackburn. 1993. A reaction diffusion model of C-N-S-O species in a stratified sediment. *Microbiol. Ecol.*, *102*, 207–215.
- Boudreau, B. P. 1984. On the equivalence of nonlocal and radial-diffusion models for porewater irrigation. *J. Mar. Res.*, *42*, 731–735.
- 1997. *Diagenetic Models and Their Implementation*, Springer-Verlag, Berlin, 417 pp.
- Emerson, S., R. Jahnke and D. Heggie. 1984. Sediment-water exchange in shallow-water estuarine sediments. *J. Mar. Res.*, *42*, 709–730.
- Furukawa, Y., S. J. Bentley, A. M. Shiller, D. L. Lavoie and P. Van Cappellen. 2000. The role of biologically-enhanced porewater transport in early diagenesis: An example from carbonate sediments in the vicinity of North Key Harbor, Dry Tortugas National Park, Florida. *J. Mar. Res.*, *58*, 493–522.
- Koretsky, C. M., C. Meile and P. VanCapellen. 2002. Quantifying bioirrigation using ecological parameters: a stochastic approach. *Geochem. Trans.*, *3*, 17–30.

Received: 7 June, 2004; revised: 21 October, 2004.